

# Is ion channel selectivity mediated by confined water?

Diego Prada-Gracia\* and Francesco Rao\*

*School of Soft Matter, Freiburg Institute for Advanced Studies, Freiburg, Germany*

E-mail: diego.prada@frias.uni-freiburg.de; francesco.rao@frias.uni-freiburg.de

## Abstract

Ion channels form pores across the lipid bilayer, selectively allowing inorganic ions to cross the membrane down their electrochemical gradient. While the study of ion desolvation free-energies have attracted much attention, the role of water inside the pore is less clear. Here, molecular dynamics simulations of a reduced model of the KcsA selectivity filter indicate that the equilibrium position of  $\text{Na}^+$ , but not of  $\text{K}^+$ , is strongly influenced by confined water. The latter forms a stable complex with  $\text{Na}^+$ , moving the equilibrium position of the ion to the plane of the backbone carbonyls. Almost at the centre of the binding site, the water molecule is trapped by favorable electrostatic interactions and backbone hydrogen-bonds. In the absence of confined water the equilibrium position of both  $\text{Na}^+$  and  $\text{K}^+$  is identical. Our observations strongly suggest a previously unnoticed active role of confined water in the selectivity mechanism of ion channels.

## 1 Introduction

Neurons enable us to think, act and remember.<sup>1</sup> At the fundamental level, an important role is played by ion channels. Forming potassium-selective pores that span the cell membrane, potassium channels are the most widely distributed channels in nature.<sup>1,2</sup> The breakthrough in the structure determination came from the identification of the bacterial homolog from *Streptomyces livi-*

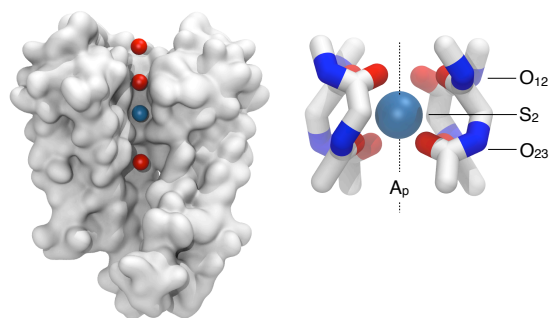


Figure 1: **The KcsA channel.** (Left) The whole protein channel.  $\text{K}^+$  ions are depicted in color (blue for the one in the S2 binding site). (Right) The reduced model of the S2 binding site, four di-glycines harmonically constrained to the crystal structure are used (see Methods for details). The experimental position of  $\text{K}^+$  at the center of the binding site, the extra and intra-cellular carbonyls are labeled as  $S_2$ ,  $O_{12}$  and  $O_{23}$ , respectively.

*dans* (KcsA).<sup>3</sup> This channel is characterized by a tetrameric structure in which four identical protein subunits associate around a central ion conducting pore. At the extracellular side, the selectivity filter is formed by a highly conserved sequence of five residues (TVGYG).<sup>3,4</sup>

Originally, the high complementarity of the selectivity filter to  $\text{K}^+$  was thought to be the reason for the selectivity.<sup>5</sup> But it is now clear that the interplay between structure and dynamics of the selectivity filter is at the origin of the mechanism.<sup>6-9</sup> Recently, atomic models of the selectivity filter were used to elucidate the role of dynamics in the

\*To whom correspondence should be addressed

process.<sup>10-13</sup> In one of these models, the filter is reduced to the most selective binding site of KcsA, called S2.<sup>14</sup> This is done by harmonically constraining the four backbone segments defining S2 to the experimental conformation.<sup>10,12</sup> Solvation free-energy calculations illustrated that the model is selective, allowing a statistical mechanics treatment of the limiting cases of rigid and very flexible binding sites.<sup>12</sup> Moreover, calculations on larger models of the filter showed that backbone fluctuations are influenced by the presence of Na<sup>+</sup> or K<sup>+</sup> at position S2.<sup>11</sup> These results support the view that several aspects of selectivity can be elucidated by analyzing ion binding to simplified models of the filter.

Another important player in selectivity is water. Simulation results showed that confined water appears together with cations in the conduction pore.<sup>15-17</sup> Notwithstanding, it is not clear yet if water actively mediates selectivity or not.

Here, the role of confined water is investigated by molecular dynamics simulations of a S2 binding site model, providing evidence that the equilibrium position of Na<sup>+</sup> within the binding site is displaced by the presence of a water molecule. Our calculations are in agreement with a recent crystallographic study<sup>18</sup> and multi-ion free-energy calculations.<sup>18,19</sup> These concepts support the idea that KcsA can bind both Na<sup>+</sup> and K<sup>+</sup> with similar strength but different mechanism.

## 2 Methods

**The S2 model.** A reduced model of the S2 binding site of the KcsA channel (PDB code: 1K4C, 1) was built with four diglycine peptides as done in Ref. 12. The heavy atoms of the reduced model were constrained with an harmonic potential of force constant  $k = 1000$  kJ/mol/nm<sup>2</sup> ( $\approx 2.4$  kcal/mol/Å<sup>2</sup>). The coordinates were translated with the vector  $(-20, 0, 0)$ , taking the axial coordinate  $A_p$  parallel to  $(1, 0, 0)$ . A pdb file of the reduced model is provided as Supplementary Information (SI).

**Molecular dynamics simulations.** All calculations were performed with the GROMACS program<sup>20,21</sup> and the AMBER-03 force field.<sup>22,23</sup> A cubic box of initial length of 4 nm solvated with

TIP4P-Ew water was used.<sup>24</sup> Simulations were integrated with the Langevin equations ( $\tau = 0.2$ ) at 300 K coupled with a Berendsen barostat ( $\tau_p = 1.0$  ps).<sup>25</sup> Long range electrostatics was computed with PME<sup>26</sup> with a 1.0 nm cut-off for all non-bonded interactions. After 10 ns of equilibration, each ion was simulated by a 100 ns long trajectory. For both Na<sup>+</sup> and K<sup>+</sup>, the starting configuration was taken as the center of the binding site ( $S_2$ , see 1). To check that there was no influence on the starting position, 20 runs of 5 ns each were further performed (Figure S1 in SI). Calculations performed with a TIP3P water model are in agreement with the present analysis (see Figure S2 in SI).

**Potential of mean force** The potential of mean force for Na<sup>+</sup> and K<sup>+</sup> was computed with GROMACS<sup>20,21</sup> along the pore axis from  $A_p = -5.0$  (the bulk) to  $A_p = 0.1$  (position  $S_2$ ). Umbrella sampling calculations were spaced by 0.1 Å along the axial coordinate  $A_p$  with the ion restrained in the normal plane with an harmonic potential ( $k_y = k_z = 1000$  kJ/mol/nm<sup>2</sup>). An additional harmonic potential of force constant  $k_x = 10000$  and 20000 kJ/mol/nm<sup>2</sup> was applied in the  $-5.0 < x < -2.1$  and  $-2.0 < x < -0.1$  range, respectively. After 1 ns of equilibration, trajectories were run for 1 ns. The weighted histogram method was used to reconstruct the potential of mean force.<sup>27</sup>

**Ion interaction energy in vacuo.** To calculate the ion interaction energy  $E_{ion}$ , the cation was harmonically restrained ( $(k_x, k_y, k_z) = (50000, 1000, 1000)$  kJ/mol/nm<sup>2</sup>) at 0.25 Å spaced positions along the axial coordinate  $A_p$  from -5.0 to 0.0 Å. After 1 ns of equilibration, each run was performed for 10 ns at 300 K and constant volume.

## 3 Results

The KcsA channel is shown in 1. In our simulation study, a reduced model of the protein selectivity filter was used. The S2 binding site was modeled by four peptides constrained to the experimental structure (right panel, see Methods for details).<sup>10,12</sup> Within this model, the pore axis centered along the channel is labeled as  $A_p$ , while the origin of the axis is taken as the experimental position of the K<sup>+</sup> ion. This position is conventionally

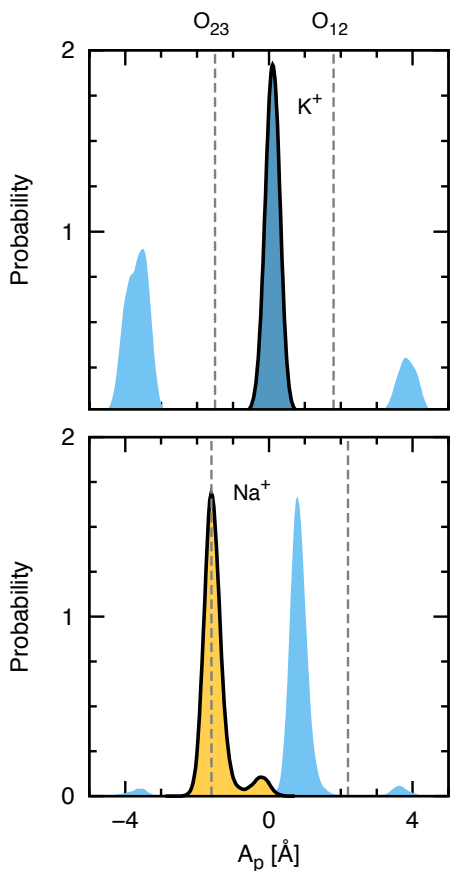


Figure 2: **Probability density functions along the pore axial coordinate  $A_p$ .** (Top)  $K^+$  (black countoured blue area); (Bottom)  $Na^+$  (black countoured orange area). Position of the closest water molecule and of  $O_{12}$  and  $O_{23}$  carbonyls are showed as blue areas and dashed lines, respectively.

called  $S_2$ . Similarly, the positions of the carbonyl oxygens defining the binding site at the extra and intra-cellular sides of the model are denoted as  $O_{12}$  and  $O_{23}$ , respectively (1).

The behavior of  $K^+$  and  $Na^+$  inside the  $S_2$  binding site was studied by molecular dynamics simulations in explicit water (see Methods for details). In both cases, the starting position of the ion was  $S_2$ . 2 shows the probability distribution of the ion position on the  $A_p$  axis. As expected,  $K^+$  was found at position  $S_2$  (black countoured blue area) between  $O_{12}$  and  $O_{23}$  (dashed lines), coordinating with the eight carbonyl oxygens of the binding site.<sup>10,14</sup>

This is not the case for  $Na^+$ . After few ns of simulation (see Figure S1 in SI), the ion hopped

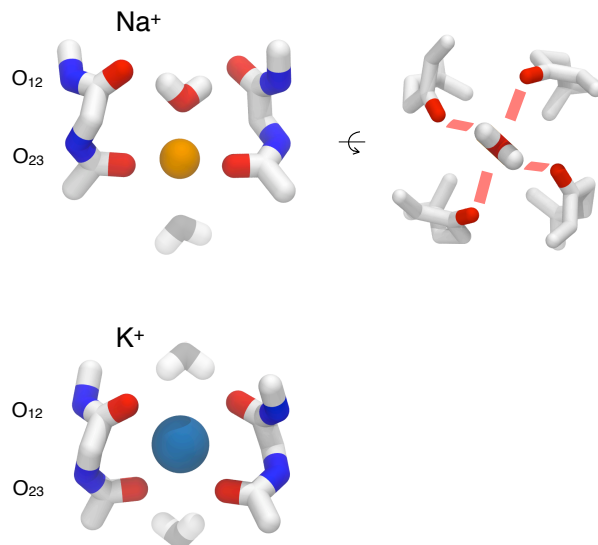


Figure 3: **Stable configurations inside the KcsA filter.** (Top)  $Na^+$  is in-plane with the  $O_{23}$  carbonyls. The presence of a confined water molecule inside the filter stabilizes this position. As shown by the 90 degrees rotated structure, this water molecule makes alternate hydrogen bonds (red thick lines) with all four  $O_{12}$  carbonyls. (Bottom)  $K^+$  is stably bound into the conventional  $S_2$  binding site. Outside the filter, one and two water molecules are present for  $Na^+$  and  $K^+$ , respectively (ghost waters).

from  $S_2$  to  $O_{23}$ , assuming a configuration perfectly in plane with the 4 carbonyl oxygens (black countoured orange area in bottom panel of 2). This position is very stable, representing the 93.6% of the total simulation time, with a high barrier to hop back to  $S_2$  (roughly four transitions in 100 ns). Analysis of the closest water molecules to the ion provided a mechanism for the configuration shift. Contrary to the case of  $K^+$  where the solvent is at the outside of the pore, one water molecule enters the channel effectively shifting the position of  $Na^+$  to  $O_{23}$ . This is shown by the probability distribution of the closest water to the ion represented as a light blue area in the figure. A structural representation of the confined water is illustrated in 3. Per se, there is no energetic preference in shifting  $Na^+$  to the  $O_{23}$  position as shown by the average interaction energy  $\Delta E_{ion}$  between the ion and the pore in vacuo (4). In the absence of water,  $S_2$  is the most stable position for both  $K^+$  and  $Na^+$ ,

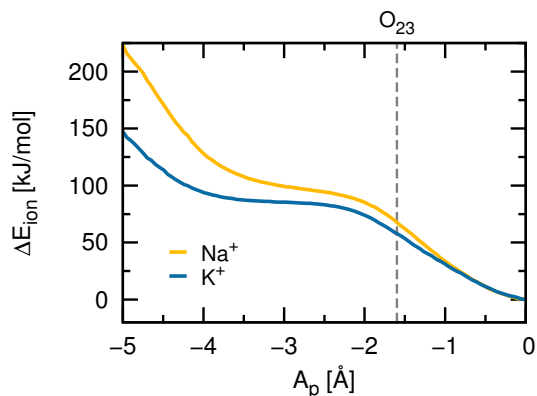


Figure 4: **Average interaction energy in vacuo** between the ion and the binding site. Data for  $\text{Na}^+$  or  $\text{K}^+$  is shown in orange and blue, respectively. The position of the  $O_{23}$  oxygen carbonyls is shown as a vertical dashed line.

strongly indicating that the binding site shift is due to the presence of a confined water.

The confined water at position  $S_2$  is stabilized by multiple strong contacts (3). The water oxygen makes electrostatic interactions with  $\text{Na}^+$ , while hydrogen bonds with two of the four carbonyls at position  $O_{12}$  are formed (3, top right panel). These hydrogen bonds are also entropically stabilized, being the confined water capable of binding to all four carbonyls of  $O_{23}$  by rotating itself around the  $A_p$  axis (bond lifetime around 2 ps, see Figure S3 in SI). This molecule is extremely stable, never exchanging with the bulk. At the outside of the channel another water molecule was found at the other side of  $\text{Na}^+$ , forming favorable electrostatic interactions with the ion (ghost water in the top panel of 3). The position of the confined water correlates with the fluctuations of  $\text{Na}^+$  around  $O_{23}$ , indicating that the ion-water configuration behaves as a complex (5). In the rare occasions when  $\text{Na}^+$  hops back to  $S_2$ , the water molecule is expelled and the complex broken ( $A_p^{\text{ion}} \approx 0$  and  $A_p^w \approx 3.8, 5$ ).

On the other hand, for the case of  $\text{K}^+$  water was only found at the outside of the pore (ghost molecules at the bottom of 3). Those waters are stabilized by the formation of hydrogen bonds with the carbonyls of the binding site. But the interaction with the ion is much weaker in this case, being the water oxygens facing the bulk.

To complement the simulation study, free-

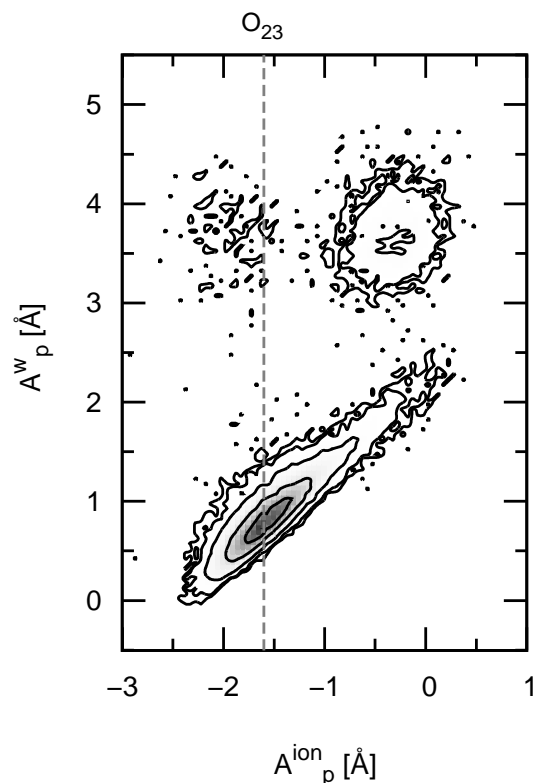


Figure 5: **2D Probability density function of the ion ( $A_p^{\text{ion}}$ ) and confined water ( $A_p^w$ ) positions for the case of  $\text{Na}^+$** . The contour lines are drawn for the probability values:  $3 \cdot 10^{-3}$ ,  $10^{-2}$ ,  $10^{-1}$ , 1.0, 4.0 and 8.0.

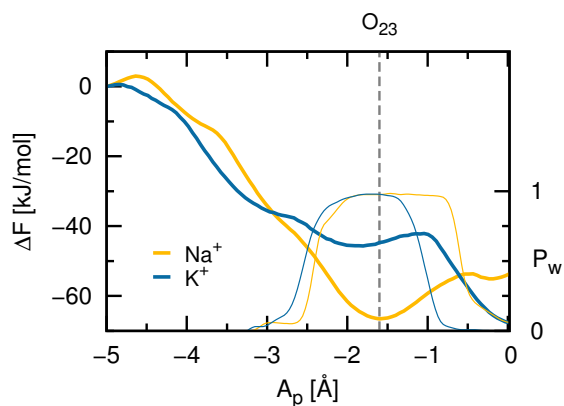


Figure 6: **Potential of mean force** for  $\text{K}^+$  and  $\text{Na}^+$  along the axial coordinate  $A_p$  (thick lines). The probability  $P_w$  to have a water molecule inside the filter is represented as thin lines. Data for  $\text{Na}^+$  or  $\text{K}^+$  is shown in orange and blue, respectively.

energy calculations were performed. In 6 the potential of mean force (PMF, see Methods) along the axial coordinate  $A_p$  is shown (thick lines). The most stable configurations for  $\text{Na}^+$  and  $\text{K}^+$  were respectively found at positions  $O_{23}$  and  $S_2$ , confirming our analysis. For both cases, position  $O_{23}$  is coupled with the presence of a water molecule inside the filter ( $P_w \approx 1$  around  $O_{23}$ , thin lines). Though energetically unfavorable,  $\text{K}^+$  at this position is in complex with a confined water as observed for  $\text{Na}^+$ . Interestingly, the free-energy difference between the outside of the pore ( $A_p = -5$ ) and the most stable binding position is remarkably similar for the two ions, indicating no strong preference towards  $\text{K}^+$  binding. These results strongly support the idea that the filter has the ability to bind both ions with different mechanisms but similar strength as already suggested in Ref.<sup>18,19</sup>

## 4 Discussion

It has been known, for more than a decade now, that the selectivity filter of KcsA presents several binding sites. Each of them forms a *cage* of optimal coordination for  $\text{K}^+$  by means of eight backbone carbonyls. Most of the calculations on KcsA selectivity were based on the relative stability of  $\text{Na}^+$  over  $\text{K}^+$  inside the pore with respect to the bulk.<sup>10,12</sup> That is, the solvation free-energy to move an ion from bulk water to a specific binding site inside the selectivity filter. These works suggested the  $S_2$  binding site as the most selective portion of the filter, being the free-energy difference in the  $S_2$  position much more favorable for  $\text{K}^+$  compared to  $\text{Na}^+$ . But this approach is not without problems if  $S_2$  is not a stable configuration for  $\text{Na}^+$ . In fact,  $\text{Na}^+$  and  $\text{K}^+$  might be characterized by distinct equilibrium positions inside the pore. X-ray crystallography<sup>18</sup> and multi-ion free-energy calculations<sup>18,19</sup> supported this idea, showing that  $\text{Na}^+$  preferentially adopts a configuration in-plane with backbone carbonyls. The observation of distinct binding positions has several consequences to our understanding of ion selectivity. Previous free-energy calculations using position restraints to the center of the binding sites need to be extended taking into account the correct equi-

librium configurations.

Our calculations on a minimalistic model of the filter provided a mechanism for the position shift. The presence of a confined water molecule in complex with  $\text{Na}^+$  effectively modifies the equilibrium configuration. The confined water is stabilized by favorable electrostatic interactions with the ion as well as multiple hydrogen-bonds with the  $O_{12}$  backbone carbonyls. The binding position shift disappears in the absence of confined water, making the latter an essential ingredient for the preferential position of  $\text{Na}^+$ . In-plane binding always implies the presence of confined water even in the unfavorable case of  $\text{K}^+$ .

In the past, water was mostly considered in terms of solvation free-energies and its screening effects without much attention to the molecular mechanism. Our results reinforce the idea that biological water is an active player at the molecular level.<sup>28</sup>

## 5 Acknowledgments

This work is supported by the Excellence Initiative of the German Federal and State Governments.

## References

- (1) Kandel, E. R.; Schwartz, J. H.; Jessell, T. M. *Principles of Neural Science*, 4th ed.; McGraw-Hill Medical, 2000.
- (2) Hille, B. *Ionic Channels of Excitable Membranes*, 3rd ed.; Sinauer Associates, 2001; Chapter 5, pp 131–168.
- (3) Doyle, D. A.; Morais Cabral, J.; Pfuetzner, R. A.; Kuo, A.; Gulbis, J. M.; Cohen, S. L.; Chait, B. T.; MacKinnon, R. *Science* **1998**, *280*, 69–77.
- (4) Heginbotham, L.; Lu, Z.; Abramson, T.; MacKinnon, R. *Biophys J* **1994**, *66*, 1061–1067.
- (5) Zhou, Y.; Morais-Cabral, J. H.; Kaufman, A.; MacKinnon, R. *Nature* **2001**, *414*, 43–48.
- (6) Fowler, P.; Tai, K.; Sansom, M. *Biophys J* **2008**, *95*, 5062–5072.

- (7) Roux, B.; Bernèche, S.; Egwolf, B.; Lev, B.; Noskov, S.; Rowley, C.; Yu, H. *J Gen Phys* **2011**, *137*, 415–426.
- (8) Dixit, P.; Asthagiri, D. *J Gen Phys* **2011**, *137*, 427–433.
- (9) Varma, S.; Rogers, D.; Pratt, L.; Rempe, S. *J Gen Phys* **2011**, *137*, 479–488.
- (10) Noskov, S. Y.; Berneche, S.; Roux, B. *Nature* **2004**, *431*, 830–834.
- (11) Asthagiri, D.; Pratt, L. R.; Paulaitis, M. E. *J Chem Phys* **2006**, *125*, 024701+.
- (12) Yu, H.; Noskov, S. Y.; Roux, B. *Proc Natl Acad Sci U S A* **2010**, *107*, 20329–20334.
- (13) Kast, S.; Kloss, T.; Tayefeh, S.; Thiel, G. *J Gen Phys* **2011**, *138*, 371–373.
- (14) Berneche, S.; Roux, B. *Nature* **2001**, *414*, 73–77.
- (15) Berneche, S.; Roux, B. *Biophys J* **2000**, *78*, 2900–2917.
- (16) Guidoni, L.; Torre, V.; Carloni, P. *FEBS Lett* **2000**, *477*, 37–42.
- (17) Domene, C.; Sansom, M. *Biophys J* **2003**, *85*, 2787–2800.
- (18) Thompson, A. N.; Kim, I.; Panosian, T. D.; Iverson, T. M.; Allen, T. W.; Nimigean, C. M. *Nat Struct Mol Biol* **2009**, *16*, 1317–1324.
- (19) Kim, I.; Allen, T. W. *Proc Natl Acad Sci U S A* **2011**, *108*, 17963–17968.
- (20) Van Der Spoel, D.; Lindahl, E.; Hess, B.; Groenhof, G.; Mark, A. E.; Berendsen, H. J. C. *J Comput Chem* **2005**, *26*, 1701–1718.
- (21) Hess, B.; Kutzner, C.; van der Spoel, D.; Lindahl, E. *J Chem Theory Comput* **2008**, *4*, 435–447.
- (22) Duan, Y.; Wu, C.; Chowdhury, S.; Lee, M. C.; Xiong, G.; Zhang, W.; Yang, R.; Cieplak, P.; Luo, R.; Lee, T.; Caldwell, J.; Wang, J.; Kollman, P. *J Comput Chem* **2003**, *24*, 1999–2012.
- (23) Sorin, E. J.; Pande, V. S. *Biophys J* **2005**, *88*, 2472–2493.
- (24) Horn, H. W.; Swope, W. C.; Pitara, J. W.; Madura, J. D.; Dick, T. J.; Hura, G. L.; Gordon, T. H. *J Chem Phys* **2004**, *120*, 9665–9678.
- (25) Berendsen, H. J. C.; Postma, J. P. M.; van Gunsteren, W. F.; DiNola, A.; Haak, J. R. *J. Chem. Phys.* **1984**, *81*, 3684–3690.
- (26) Darden, T.; York, D.; Pedersen, L. *J Chem Phys* **1993**, *98*, 10089–10092.
- (27) Kumar, S.; Rosenberg, J.; Bouzida, D.; Swendsen, R.; Kollman, P. *J Comp Chem* **1992**, *13*, 1011–1021.
- (28) Ball, P. *Nature* **2011**, *478*, 467–468.